Growth-Melt Asymmetry in Crystals and Twelve-Sided Snowflakes

A. Cahoon,[1] M. Maruyama,[2] and J. S. Wettlaufer[1,3]
[1]Department of Physics, Yale University, New Haven, Connecticut, 06520, USA
[2]Department of Physics, Osaka City University, Osaka, 558-8585, Japan
[3]Department of Geology and Geophysics, Yale University, New Haven, Connecticut, 06520, USA
(Received 19 January 2006; published 29 June 2006)

It is in the lexicon of crystal growth that the shape of a growing crystal reflects the underlying microscopic architecture. Although it is known that in weakly nonequilibrium conditions the slowest growing orientations ultimately dominate the asymptotic shape, is the same true for melting? Here we observe and show theoretically that while the two-dimensional steady melt shapes of ice are bounded by six planes, these planes are not proper facets but instead are rotated 30 degrees from the prism planes of ice. Finally, the transient melting state exposes 12 apparent crystallographic planes thereby differing substantially from the transient growth state.

DOI: 10.1103/PhysRevLett.96.255502 PACS numbers: 81.10.Aj, 05.70.Np, 64.70.Dv, 89.75.Kd

The relationship between growth, form and structure is vividly illustrated in crystalline matter, and snowflakes provide one of the most familiar and compelling examples. Whether a crystal grows in the laboratory under controlled conditions or in a natural setting, one recognizes the basic material through the symmetry of the shape. Despite the fact that in modern parlance the snowflake is an icon for nonlinear pattern formation in systems driven away from equilibrium, understanding the mechanisms by which the microscopic constituents (water molecules) influence the macroscopic shape still forms an active area of inquiry. The scientific study of such problems of growth and form dates to Hooke, Kepler, and Descartes [1,2]; compilations of photographs of natural and artificial snowflakes [3,4] reveal both complexity and commonality. The allure of the shapes of snowflakes has long captured the imagination of artists, laypersons, and scientists alike; their importance lies both in their beauty and in their ubiquity.

Understanding the underlying tenets of crystal growth and surface thermodynamics in all materials is a major goal of condensed matter science, and the considerable breadth of applicability of ice phenomena (e.g., Ref. [5]) draws attention to fundamental questions. In *equilibrium* a three dimensional crystal at absolute zero is fully faceted (molecularly smooth) because the energy required to form a vacancy or adatom cannot be compensated by entropy of configuration. As the temperature rises entropy comes into prominence and a smooth orientation can become molecularly rough. Thus, it is known from experimental studies as well as microscopic and mean-field theory that an ideal, dislocation-free, equilibrium crystal shape depends on temperature: it is fully faceted at absolute zero, and becomes more rounded, or locally rough, as its temperature increases [6]. Upon consideration of the dominant intermolecular interactions in a material, the bond energies can be estimated, and hence one can build a picture of the surface free energy of a crystal, $\gamma(\hat{\mathbf{n}})$, as the sum of the energies of all the bonds broken per unit area in the creation of the surface of an orientation $\hat{\mathbf{n}}$ relative to the underlying crystalline lattice. The geometric Wulff construction determines the equilibrium crystal shape through a minimization of $\gamma(\hat{\mathbf{n}})$ [7–12]. Through independent control of temperature and pressure, the entire range of equilibrium shapes, from fully faceted to completely rough and rounded, has been observed in ice [13].

Weakly driven growth forms evolving from partially faceted equilibrium shapes become more faceted during growth [7,13–19]. This growth induced polygonalization originates in the fact that the accretion of material normal to facets is an activated process whereas no nucleation barrier exists for rough orientations which grow rapidly and thereby leave behind the slowly moving facets to dominate the shape. Although the intuition gleaned from the Wulff shape can be applied to conditions of weak disequilibrium [16,18], a similar construction on the anisotropic velocity, due to Frank [14] and Chernov [15] can, depending on the initial conditions, produce the steady state growth shape. Nonetheless, the relation between *equilibrium* and *growth* or *melt* shapes is much less concrete than appears to be widely appreciated [20,21]. We demonstrate experimentally and theoretically that no direct analogy to the Frank-Chernov construction exists for melting and that it is the asymmetry between the kinetics of growth and those of melting that is responsible. A novel consequence of this is an ''apparent rotation'' of the crystallographic axes during transient melting, the route to which involves a sixfold crystal becoming 12-fold and then sixfold again.

A common feature of the iconoclastic six-sided dendritic stars (crystals growing perpendicular to the crystallographic c axis) is their fully faceted solid hexagonal core. Frank [2] made the important point that the vast swath of growth morphologies exhibited by vapor grown crystals can only be explained by mechanisms that do not rely on dislocations, which are largely absent. We have therefore chosen the simplest model system for which purity is easily

maintained and growth conditions are finely controlled: single, dislocation-free, ice crystals grown from their melts. In particular, we use a high-pressure temperature-controlled anvil cell [22] to study hexagonal morphologies in their essence; near the roughening transitions of the prism planes under conditions of weak disequilibrium.

The sequence of growth and melt shapes in Fig. 1 displays the entire process. The high-pressure anvil cell is immersed in a temperature-fixed alcohol bath, but we have modified the original apparatus, described in Ref. [22], so that during melting the temperature is raised at a constant rate using a heater wound around a lower anvil. The sequence is as follows: (a) In the first panel of Fig. 1 we show an initial, near equilibrium, shape that is nearly fully faceted with the sixfold symmetry. (b) When melting is initiated at a small drive, $\frac{\Delta\mu}{k_bT} \ll 1$, only the corners are melted and the facets are pinned. (c), (d), (e) Rough orientations in the corners evolve into planar surfaces and thus transient 12-sided shapes appear. (f), (g), (h) The roughest orientations gradually dominate the melt shape with sixfold symmetry, but these surfaces are slightly curved noncrystallographic planes. (i) Growth begins at rough orientations. (j), (k) Transient rounded shapes are seen in contrast to 12 sides seen during melting. (l), (m), (n), (o) Fast growing rough surfaces grow out into the corners, leaving pinned facets behind, as described previously [19,20,23–25].

Our physical interpretation, which quantifies our previous heuristic theory [20], is as follows. When melting is initiated the weakly bound corner molecules can respond immediately and depart the solid. Thus we observe the normal motion of facets to be small compared to rough orientations; the latter moving approximately 15% of the characteristic crystal size while the former does not move a discernible distance. However, in contrast to growth, the motion of a finite facet during melting is not an activated process. The melt rate of an infinite dislocation-free facet is limited by the nucleation rate of ''negative islands''. A finite facet differs; molecules detach from the terrace edges and the facet recedes towards its center, uncovering the layer below to repeat the process. Hence, the monolayers bounding the prism facets recede from the corners. Once a corner molecule departs, it exposes a new corner, and thereby the process repeats. The ratio of the rate of corner formation to the rate of recession of the monolayer across the facet determines the slope of the surface. Clearly visible is the formation of a 12-sided transient state which gives way to a six-sided, apparently faceted, state in which each ''facet'' appears perpendicular to an a axis; a corner on the equilibrium shape. It thus *appears* as though the crystal has rotated by 30 degrees. That the rotation is cosmetic is demonstrated when growth is initiated because the facets on the melt shape are dynamically determined as described above, and are, in fact, molecularly rough. During growth they move rapidly to reverse the process and restore the faceted equilibrium crystal to its original state [19,20,23–25].

When the motion of the phase boundary is limited by local interfacial processes, it can be modeled as *geometric* in the sense that the normal velocity V at an interfacial point depends on the *shape* and *position* of the interface, and not on field variables modified by the interface motion or long-range diffusion in the bulk (see, e.g., Refs. [23,24]). Whether a crystal is growing or melting, the interface evolves with a normal velocity that is governed by the physical kinetics of the surface. In general, the evolution of an interface is given by

$$\left(\frac{\partial \vec{C}(u,\tau)}{\partial \tau}\right)_u = -V\hat{n}, \tag{1}$$

where $\vec{C}(u,\tau)$ is a point on the surface parametrized by u at time τ and $\hat{n}$ is the inward-pointing normal. This explicitly connects the geometry of the macroscopic shape to the governing microphysics through V, the functional form of which is constrained by the surface kinetics within the geometric approach; $V = V(\theta, \Delta\mu)$. It is convenient [23,24] to reparametrize Eq. (1) by the angle θ between the positive x axis and the unit tangent to the surface $\hat{t}$. Thus, the orientation dependence of V captures the transition in the kinetics from faceted orientations, where V_F is the normal velocity, to rough orientations, where V_R is the normal velocity, through

$$V(\theta,\Delta\mu) = V_F(\theta,\Delta\mu)\xi(\theta) + V_R(\theta,\Delta\mu)[1-\xi(\theta)], \tag{2}$$

and $\xi(\theta)$ models the transition between them. Equation (1) can be solved by the method of characteristics [23–25] to yield the trajectory of a surface orientation as

$$\vec{C}(\theta,\tau) = \vec{C}_0(\theta) + [-V(\theta)\hat{n} + V'\hat{t}]\tau, \tag{3}$$

where $V' \equiv \frac{\partial V}{\partial \theta}$.

We initialize our model with the smooth shape shown in Fig. 1(a) which contains all orientations. As it reaches a 12-fold state, many orientations have been eliminated. Essentially, what was a corner of orientations spanning $\pi/3$ rapidly becomes a nearly flat segment spanning $|\delta\theta| \ll \pi/3$. As a result the melt shapes are controlled by the ratio of the velocity at the roughest orientations to the velocity at the facet orientations. We extract the normal velocity from the experimental images; its polar plot outlines a petaled flower with the same symmetry as the crystal. The measured $V(\theta)$ are then fit to a function of the form of Eq. (2) and employed in Eq. (3) to predict the crystal's shape at later times. Without imposing restrictions on $\xi(\theta)$ and $V_R(\theta)$, Eq. (2) is quite general.

Here, we take the simplest model for Eq. (2) that preserves the symmetry of the crystal:

$$\xi(\theta) = \cos^2(3\theta) \quad \text{and} \quad V_R(\theta) = v_R + b\cos^2(3\theta), \tag{4}$$

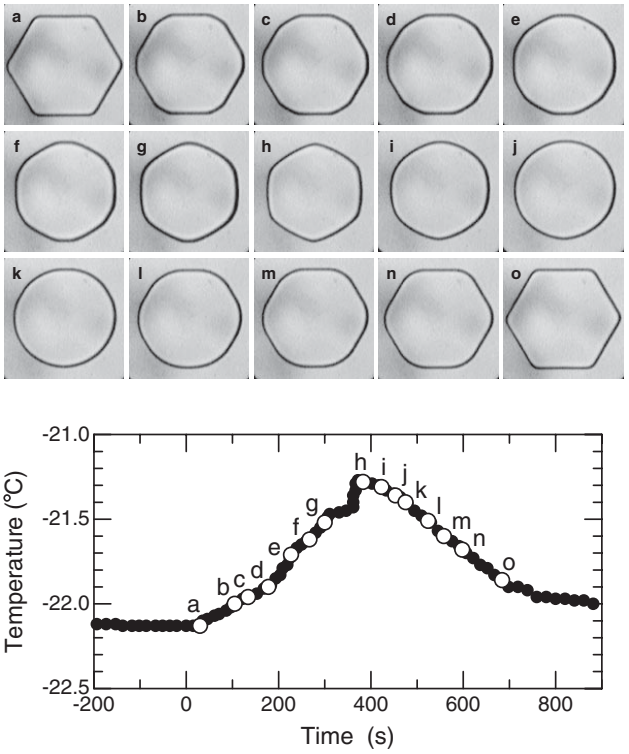

FIG. 1. In the top panel we show a sequence of melting and growth shapes observed in a high-pressure anvil cell modified from Ref. [22]. The cell has a constant volume of about 0.01 cm^3 and the scale of an individual frame is 0.5 mm. The pressure is held at 2000 bar and hence the bulk coexistence temperature is $-22\,^{\circ}C$, which is measured with a Chromel-Constantan thermocouple. The system's temperature, T, and pressure, p, are controlled along a line that is parallel to the bulk coexistence line and we can change the crystal shape by fine control of $\frac{\Delta\mu}{k_bT} \ll 1$, where $\Delta\mu$ is the departure of the chemical potential from bulk coexistence. Accordingly, the pressure is continuously varied due to the difference in volume between the phases, and if T is held constant the ice crystal takes its equilibrium shape with a constant volume. The axis of observation is parallel to the crystallographic c axis, and hence each corner is colinear with one of the a axes and the six prism facets are clearly visible. The sequence, which takes 700 seconds, is described in detail in the text. In the lower panel we show the temperature data with the circles (labeled a–o) corresponding to the upper panel; the warming or cooling rate determines a driving force that we estimate from observed melt-growth rates of rough orientations to be $\frac{\Delta\mu}{k_bT} \approx 10^{-7}$.

where v_R is the velocity at the roughest orientations and b provides a measure of the curvature of the polar plot of V and is given by the relation $V''(\theta = \pi/2) + V''(\theta = 0) = 36b$, where $V'' \equiv \frac{\partial^2 V}{\partial\theta^2}$. Finally, we note that $V_F(\theta_F, \Delta\mu)$ is implicitly solely defined at facet orientations θ_F where it then depends solely on $\Delta\mu$. Therefore, there are three parameters in our model for V:V_F, v_R, and b. Using this in Eq. (3), we reproduce the main observations: (i) the melt process results in a crystal with an apparent reorientation of axes, (ii) the corners evolve with decreasing curvature, and (iii) the transient melt shape is a 12-sided figure (see Fig. 2). The distinction between melting and growth is clearly demonstrated by the difference in the model velocity parameters; there is no time reversal symmetry in the equation of motion (1) that can capture the dynamics of a partially faceted crystal.

An alternative description of the melt process written in terms of the surface curvature κ, and successful in growth studies [19,24,25], provides further insight into the melting process. When κ is a function of θ a local evolution equation can be derived,

$$\frac{\partial\kappa}{\partial\tau} = -\kappa^2\tilde{V}, \tag{5}$$

where $\tilde{V} \equiv V + V''$. Here, the sign of $\tilde{V}$ controls whether the curvature increases or decreases. The solution to Eq. (5) is

$$\kappa(\theta, \tau) = \frac{\kappa_0}{1 + \tilde{V}(\theta)\kappa_0\tau}, \tag{6}$$

where $\kappa_0 = \kappa_0(\theta, \tau = 0)$. Hence, in principal, the curvature can diverge; every orientation with negative $\tilde{V}$ could reach infinite curvature in finite time. As was proved for the case of growth [25], curvature divergence in melting is preempted by the loss of ''dangerous'' orientations which melt to the facet edge before the critical time. The loss occurs through the initiation of a shock at a time corresponding to the minimum time for curvature divergence; the shock consumes the orientations faster than they can

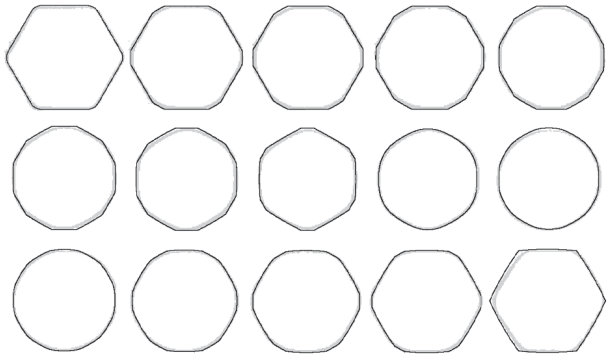

FIG. 2. Comparison of theory with experiment for the melt and growth sequence a–o of Fig. 1. The digitized experimental images are shown (light lines) overlain with the theoretical model (dark lines) as given by using $V(\theta) = V_F\cos^2(3\theta) + [v_R + b\cos^2(3\theta)][1 - \cos^2(3\theta)]$ in Eq. (3), where for melting, in units of v_R (or in units of $\mu m\,s^{-1}$), the parameters $v_R = 1$, $V_F = 0.07$, $b = -0.009$ ($v_R = 0.11$, $V_F = 0.008$, $b = -0.001$) are extracted from the initial shape. In the calculations V is maintained as positive definite and hence during melting we let $V \rightarrow -V$ in the above equations by changing the sign of the parameters. For *growth* $v_R = 0.12$, $V_F = 0.016$, $b = 0.12$ in $\mu m\,s^{-1}$ thereby displaying the microscopic origin of the difference between growth and melting.

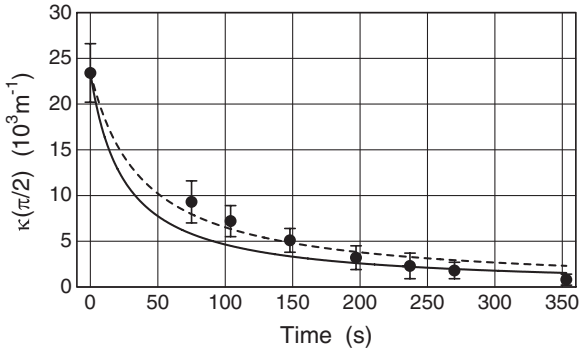

FIG. 3. We plot the measured curvature at $\theta = \pi/2$ for the melt sequence a–h of Fig. 1. The data (closed circles) are fit to a function of the form $A/(1 + Bt)$ (dashed line, where $A/10^3 = 23.5 \pm 1.1\ \mathrm{m}^{-1}$ and $B = 0.026 \pm 0.004\ \mathrm{s}^{-1}$) and are compared to the theoretical prediction (solid line) determined by inserting the velocity model used to calculate the melt shapes in Fig. 2 into Eq. (6).

blow up. We measure the curvature directly from the experimental sequence and calculate the expected curvature from our model. The agreement is demonstrated in Fig. 3. Finally, we note an important and fortuitous aspect of a geometric theory of melting is that as the crystal melts the validity of the geometric assumptions increases. The surface area of a melting crystal continuously decreases thereby reducing the effect of latent heat on the local conditions of disequilibrium. Such an effect depends on the surface state, and we estimate that as the facet size becomes small compared to the circumference, a geometric model provides an increasingly accurate description. This explains the close agreement between our model and experiment.

We have examined the basic relationships between *equilibrium* and *growth* or *melt* shapes to find that there is an asymmetry between growth and melting that has a fundamental origin in the kinetics of molecular attachments and detachments at the surface. We have used a high-pressure, temperature-controlled optical cell to observe that while the ostensibly two-dimensional steady melt shapes of ice are bounded by six planes, the planes themselves are not proper facets but instead are rotated 30 degrees from the prism planes of ice. Therefore, the similarity with faceted growth shapes is solely cosmetic. Finally, we find that the transient melting state exposes 12 apparent crystallographic planes and thereby differs substantially from the transient growth state. We have described these processes quantitatively using a geometric theory for the melt shape evolution. The results are basic to the growth and melting of all solids and are of geophysical relevance due to the ubiquity of ice crystal growth in the Earth's bodies of water and throughout its atmosphere.

We acknowledge the support of the Bosack and Kruger Foundation, the National Science Foundation, the Japan Society for the Promotion of Science, and Yale University. J. S. W. thanks Trinity College and the Department of Applied Mathematics and Theoretical Physics, University of Cambridge, for support during the sabbatical leave where this paper was written.

[1] R. Descartes, "Les Météores," published with "Discours de la Méthode" by Ian Maire Leiden, in *Oeuvres de Descartes*, edited by C. Adam and P. Tannery (Léopold Cerf, Paris, 1902), Vol. 6, pp. 293–308.
[2] F. C. Frank, Contemp. Phys. **23**, 3 (1982).
[3] U. Nakaya, *Snow Crystals: Natural and Artificial* (Harvard University Press, Cambridge, MA, 1954).
[4] Y. Furukawa, Chemie in Unserer Zeit **31**, 58 (1997).
[5] *Ice Physics and the Natural Environment*, edited by J. S. Wettlaufer, J. G. Dash, and N. Untersteiner, NATO ASI, Series I, Vol. 56 (Springer-Verlag, Heidelberg, 1999).
[6] S. Balibar, H. Alles, and A. Y. Parshin, Rev. Mod. Phys. **77**, 317 (2005).
[7] G. Wulff, Z. Krystallogr. Mineralogie **34**, 449 (1901).
[8] A. Dinghas, Z. Kristallogr., Kristallgeom., Kristallphys., Kristallchem. **105**, 304 (1944).
[9] L. D. Landau, *Collected Papers of L.D. Landau* (Pergammon, Oxford, 1965), pp. 540–545.
[10] C. Herring, Phys. Rev. **82**, 87 (1951).
[11] J. W. Cahn and W. C. Carter, Metall. Mater. Trans. A **27**, 1431 (1996).
[12] S. Kodambaka, S. V. Khareb, I. Petrova, and J. E. Greene, Surf. Sci. Rep. **60**, 55 (2006); S. V. Khare, S. Kodambaka, D. D. Johnson, I. Petrov, and J. E. Greene Surf. Sci. **522**, 75 (2003).
[13] M. Maruyama, Y. Kishimoto, and T. Sawada, J. Cryst. Growth **172**, 521 (1997).
[14] F. C. Frank, in *Growth and Perfection of Crystals*, edited by R. H. Doremus, B. W. Roberts, and D. Turnbull (Wiley, New York, 1958), pp. 411–419.
[15] A. A. Chernov, Sov. Phys. Crystallogr. **7**, 728 (1963).
[16] J. Villain, Nature (London) **350**, 273 (1991).
[17] B. Berge, L. Faucheux, K. Schwab, and A. J. Libchaber, Nature (London) **350**, 322 (1991).
[18] J. Flesselles, M. O. Magnasco, and A. J. Libchaber, Phys. Rev. Lett. **67**, 2489 (1991).
[19] M. Maruyama, N. Kuribayashi, K. Kawabata, and J. S. Wettlaufer, Phys. Rev. Lett. **85**, 2545 (2000).
[20] M. Elbaum and J. S. Wettlaufer, Phys. Rev. E **48**, 3180 (1993).
[21] F. C. Frank and M. B. Ives, J. Appl. Phys. **31**, 1996 (1960).
[22] M. Maruyama, J. Cryst. Growth **275**, 598 (2005).
[23] J. E. Taylor, J. W. Cahn, and C. A. Handwerker, Acta Metall. Mater. **40**, 1443 (1992).
[24] J. S. Wettlaufer, M. Jackson, and M. Elbaum, J. Phys. A **27**, 5957 (1994).
[25] V. Tsemekhman and J. S. Wettlaufer, Stud. Appl. Math. **110**, 221 (2003).